DOI: 10.37863/umzh.v73i8.333

UDC 517.5

R. Jedynak, J. Gilewicz (K. Pulaski Univ. Technology and Humanities, Radom, Poland)

DISTRIBUTIONS OF ZEROS AND POLES OF N-POINT PADÉ APPROXIMANTS TO COMPLEX-SYMMETRIC FUNCTIONS DEFINED AT COMPLEX POINTS

РОЗПОДІЛ НУЛІВ І ПОЛЮСІВ N-ТОЧКОВИХ НАБЛИЖЕНЬ ПАДЕ КОМПЛЕКСНО-СИМЕТРИЧНИХ ФУНКЦІЙ, ВИЗНАЧЕНИХ У КОМПЛЕКСНИХ ТОЧКАХ

The knowledge of the location of zeros and poles Padé and N-point Padé approximations to a given function f provides much valuable information about the function being studied. In general PAs reproduce the exact zeros and poles of considered function, but, unfortunately, some spurious zeros and poles appear randomly. Then, it is clear that the control of the position of poles and zeros becomes essential for applications of Padé approximation method. The numerical examples included in the paper show how necessary for the convergence of PA is the knowledge of the position of their zeros and poles. We relate our research of localization of poles and zeros of PA and NPA in the case of Stieltjes functions because we are interested in the efficiency of numerical application of these approximations. These functions belong to the class of complex-symmetric functions. The PA and NPA to the Stieltjes functions in different regions of the complex plane is also analyzed. It is expected that the appropriate selection of the complex point for the definition of approximant can improve it with respect to the traditional choice of $\zeta = 0$. All considered cases are graphically illustrated. Some unique numerical results presented in the paper, which are sufficiently regular should motivate the reader to reflect on them.

Знання про місцезнаходження нулів і полюсів наближень Паде та N-точкових наближень Паде для даної функції f надає дуже важливу інформацію щодо цієї функції. Взагалі, наближення Паде повторюють точні нулі та полюси функції, але, на жаль, можуть з'являтись інші нулі та полюси. Зрозуміло, що контроль позиції нулів і полюсів є важливим для застосувань методу наближень Паде. Числові приклади, що наведені у роботі, демонструють необхідність знати позицію нулів і полюсів для того, щоб гарантувати збіжність наближення Паде. Наші дослідження позиції полюсів і нулів наближень Паде та N-точкових наближень Паде виконано для функцій Стільтьєса, оскільки нас цікавлять ефективні числові застосування таких наближень. Ці функції належать до класу комплексно-симетричних функцій. Також досліджено наближення Паде та N-точкові наближення Паде для функцій Стільтьєса у різних регіонах комплексної площини. Очікується, що правильний вибір комплексної точки для визначення наближення може покращити її відносно стандартного вибору $\zeta = 0$. Для всіх розглянутих випадків надано відповідні ілюстрації. Деякі наведені у статті унікальні числові результати є достатньо типовими й повинні спонукати читача замислитися над ними.

1. Introduction. In the paper published in 1976 by Chisholm et al. [2], the authors claimed that all poles and zeros of diagonal Padé approximants (PAs) $[n/n]$ to $\ln(1-z)$ developed at the complex point ζ interlace on the cut $\zeta + t(1-\zeta),\ t \in]1, \infty[$. Klarsfeld remarked in 1981 [7] that the zeros do not follow this rule. The study of this problem was the starting motivation of two Ph.D. theses directed by the second author [5, 8]. The primary theoretical results obtained from these theses were published in [6]. However, some interesting numerical observations remain unexplained. Some of these open problems are presented in this paper.

The paper is organized as follows. In Section 2, we recall the basic terminology related to PAs, complex-symmetric functions and Stieltjes functions. We also summarize the classical results of the location of the zeros and poles of PAs to the Stieltjes functions. In Section 3, we discuss the distribution of the zeros and poles of PAs in a few cases of the development points of PAs to $\ln(1-z)$ and $-\dfrac{1}{z}\ln(1-z)$. Section 4 contains a theorem which describes the location of the zeros and poles

of PAs at complex and complex conjugate points. Section 5 provides the appropriate theorems to N-point Padé approximants (NPAs) of the complex-symmetric functions. In Section 6, we describe numerical observations related to the specific location of zeros and poles of PAs. The problem of convergence of PA is also considered. Finally, the conclusion contains some concluding remarks. At the end of the paper, there is an Appendix. It includes the extra material on the problems discussed in the main party of the manuscript. The paper is illustrated with various numerical examples, mainly in the form of graphs, to introduce the reader to the problems discussed in the relevant sections.

2. PA, complex-symmetric functions and Stieltjes functions. Let f be an analytic function having at the points $\zeta_1, \ldots, \zeta_N \in \mathbb{C}$ the power expansions:

$$C_i(z) = \sum_{k=0}^{p_i-1} c_k^i (z-\zeta_i)^k + O\Big((z-\zeta_i)^{p_i}\Big), \quad i = 1, \ldots, N.$$

Then the NPA $[m/n]$ to f at the points $\zeta_1, \ldots, \zeta_N \in \mathbb{C}$ noted [11]

$$[m/n]^{p_1 p_2 \ldots p_N}_{\zeta_1 \zeta_2 \ldots \zeta_N}(z) = \frac{P_m(z)}{Q_n(z)} = \frac{a_0 + a_1 z + \ldots + a_m z^m}{1 + b_1 z + \ldots + b_n z^n},$$

where

$$m + n + 1 = p = p_1 + p_2 + \ldots + p_N$$

is defined by

$$f(z) - [m/n](z) = O\Big((z-\zeta_i)^{p_i}\Big), \quad i = 1, 2, \ldots, N. \tag{1}$$

We always suppose that it exists and then (1) leads to

$$Q_n(z) f(z) - P_m(z) = O\Big((z-\zeta_i)^{p_i}\Big), \quad i = 1, 2, \ldots, N,$$

representing $m + n + 1$ linear equations for unknowns $a_0, a_1, \ldots, a_m, b_1, \ldots, b_n$. If $N = 1$ this reduces to the classical one-point PA. A compact formula giving this PA at $z = 0$ is as follows:

$$\frac{P_m(z)}{Q_n(z)} = \frac{\begin{vmatrix} C_{(m)}(z) & zC_{(m-1)}(z) & z^2 C_{(m-2)}(z) & \ldots & z^n C_{(m-n)}(z) \\ c_{m+1} & c_m & c_{m-1} & \ldots & c_{m-n+1} \\ c_{m+2} & c_{m+1} & c_m & \ldots & c_{m-n+2} \\ \vdots & \vdots & \vdots & \vdots & \vdots \\ c_{m+n} & c_{m+n-1} & c_{m+n-2} & \ldots & c_m \end{vmatrix}}{\begin{vmatrix} 1 & z & z^2 & \ldots & z^n \\ c_{m+1} & c_m & c_{m-1} & \ldots & c_{m-n+1} \\ c_{m+2} & c_{m+1} & c_m & \ldots & c_{m-n+2} \\ \vdots & \vdots & \vdots & \vdots & \vdots \\ c_{m+n} & c_{m+n-1} & c_{m+n-2} & \ldots & c_m \end{vmatrix}},$$

where

$$C_{(k)}(z) = \begin{cases} \sum_{j=0}^{k} c_j z^j & \text{if } k \geq 0, \\ 0 & \text{otherwise.} \end{cases}$$

The doubly infinite array of PA is called Padé table

m	n			
	0	1	2	...
0	$[0/0]$	$[0/1]$	$[0/2]$	...
1	$[1/0]$	$[1/1]$	$[1/2]$	...
2	$[2/0]$	$[2/1]$	$[2/2]$	...
⋮	⋮	⋮	⋮	⋮

The first column in this table contains the truncated power series. In this paper, we are concerned by PA to the Stieltjes functions

$$f(z) = \int_0^{1/R} \frac{d\mu(t)}{1-tz}, \quad d\mu \geq 0, \quad R \geq 0, \quad z \in \mathbb{C} \setminus [R, \infty[, \tag{2}$$

which belong to the largest class of *complex-symmetric functions*, i.e., functions satisfying the condition

$$f(\overline{z}) = \overline{f(z)}. \tag{3}$$

In particular, if ζ and $\overline{\zeta}$ are two complex conjugate points, then

$$f(z) = \sum_{n=0}^{\infty} c_n (z-\zeta)^n \quad \text{and} \quad f(z) = \sum_{n=0}^{\infty} \overline{c_n} (z-\overline{\zeta})^n.$$

Classical results [3]:

1. All poles and zeros of PA $[n-1/n]$ and $[n/n]$ to the Stieltjes functions (2) at $z=0$ interlace on the cut $]R, \infty[$. This property is illustrated in Fig. 1. It is due to a fact that the numerators and denominators of these PA are related to the orthogonal polynomials $\overline{P}$ and $\overline{Q}$ by $\overline{P_n(x)} = x^n P_n(1/x)$ and $\overline{Q_n(x)} = x^n Q_n(1/x)$, respectively. The zeros of the orthogonal polynomials are located inside of the support of the measure defining those polynomials.

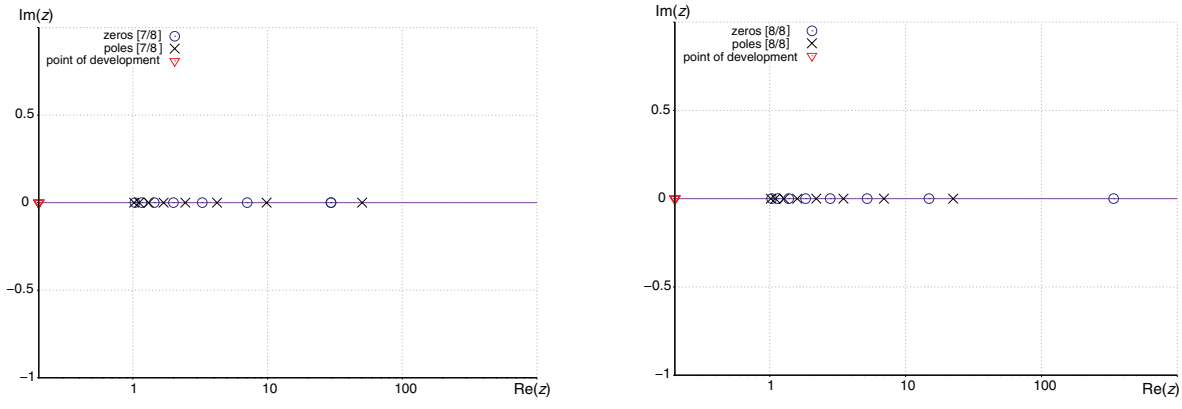

(*a*) (*b*)

Fig. 1. Distributions of zeros and poles of (*a*) PA $[n-1/n]$ and (*b*) PA $[n/n]$ for $n=8$ to $-\frac{1}{z}\ln(1-z)$ at $z=0$ which are plotted on a semi-logarithmic scale. They interlace on the cut $]R, \infty[$.

2. The sequences of these diagonal and subdiagonal PA converge uniformly to the Stieltjes function in $C[R, \infty[$.

3. Let us consider the set $\{[n\lambda/n]\}$ of PA on the sloping diagonal λ. Fig. 2 (*a*) presents the distributions of zeros $[n\lambda/n]$ to the Stieltjes function $\left(-\frac{1}{z}\ln(1-z)\right)$ for three cases of $\lambda = \{10, 100, 1000\}$. We observe that with the increase of this parameter those points tend to the circle of convergence. We also examine the impact of n when the parameter λ is set. Fig. 2 (*b*) shows the distributions of zeros for $\lambda = 4$ and $n = \{2, 4, 8\}$. They look very similar to each other. $\lambda = \infty$ corresponds to the PA $[n/0]$ and $\lambda = 1$ to the diagonal PA $[n/n]$. All zeros of PA $[n/0]$ are located in the vicinity of the circle of convergence of the Taylor series of the Stieltjes function. This property is documented in Fig. 2 (*c*). If λ $(1 < \lambda < \infty)$ decreases to 1 $(\lambda \to 1)$, the zeros of PA remove from the circle of convergence increasing the region of convergence D_λ of PA limited by the position of zeros (see Fig. 1). The exceeding zeros, i.e., $n\lambda - n$ zeros which are not located on the cut, put away, surrounding the cut, and (or) go to infinity. This problem was first studied by Baker [1], but his formula (16.10) is false: $\frac{\lambda-1}{\lambda+1}$ must be replaced by $\frac{\lambda-1}{2}$ which changes the result radically. The correct limits of these regions were given in [3, p. 267].

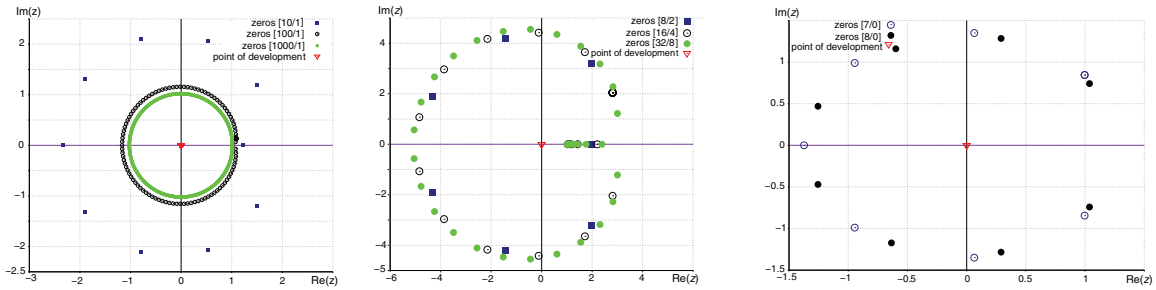

(*a*) (*b*) (*c*)

Fig. 2. Distributions of zeros of (*a*) PA $[\lambda n/n]$ for $\lambda = \{10, 100, 1000\}$ to $-\frac{1}{z}\ln(1-z)$ at $z = 0$, (*b*) PA $[4n/n]$ for $n = \{2, 4, 8\}$ to $-\frac{1}{z}\ln(1-z)$ at $z = 0$, and (*c*) PA $[n/0]$ for $n = \{7, 8\}$ to $-\frac{1}{z}\ln(1-z)$ at $z = 0$.

These results show how necessary for the convergence of PA is the knowledge of the position of their zeros and poles. In general PAs reproduce the exact zeros and poles of considered function, but, unfortunately, some spurious zeros and poles appear randomly. Then it is clear that the control of the position of poles and zeros becomes essential for applications of PA method. Some beautiful theorems of convergence of PA outside the set of measure zero or of capacity zero are inapplicable in practice because these sets are not localizing. Since we are interested in the efficiency of the numerical application of PA, we relate here our research of localization of poles and zeros of PA in the case of Stieltjes functions. We also analyze the quality of PA to the Stieltjes functions in different regions of the complex plane expecting that the appropriate choice of the complex point for the definition of PA can improve it with respect of the traditional choice of $\zeta = 0$.

At the end of this section, we shortly present the example of using the method mentioned before of location zeros of PA to the inverse Langevin function which is a complex-symmetric one, but it is not related to the Stieltjes function. It is an essential function because it is extensively used in magnetism and polymer physics. In papers [12 – 14], we derived different approximation formulas to that function. We evaluated the radius of the convergence of the Taylor series of the inverse Langevin

function by the procedure by Mercer and Roberts and obtained value $r = 0.904$ for 1500 nonzero coefficients of the Taylor series expansion. Below we present the truncated Taylor series expansion of this function

$$\mathcal{L}^{-1}(x) = 3x + \frac{9x^3}{5} + \frac{297x^5}{175} + \frac{1539x^7}{875} + O\left(x^9\right).$$

It can be transformed to more convenient form for numerical computations

$$f(x) = \frac{1-x^2}{3x}\mathcal{L}^{-1}(x) = 1 - \frac{2x^2}{5} - \frac{6x^4}{175} + \frac{18x^6}{875} + O\left(x^9\right).$$

Fig. 3 presents the distributions of zeros of PA $[4n/n]$ to those mentioned before functions for $n = \{25, 50, 75\}$. Both functions have the same radius of convergence.

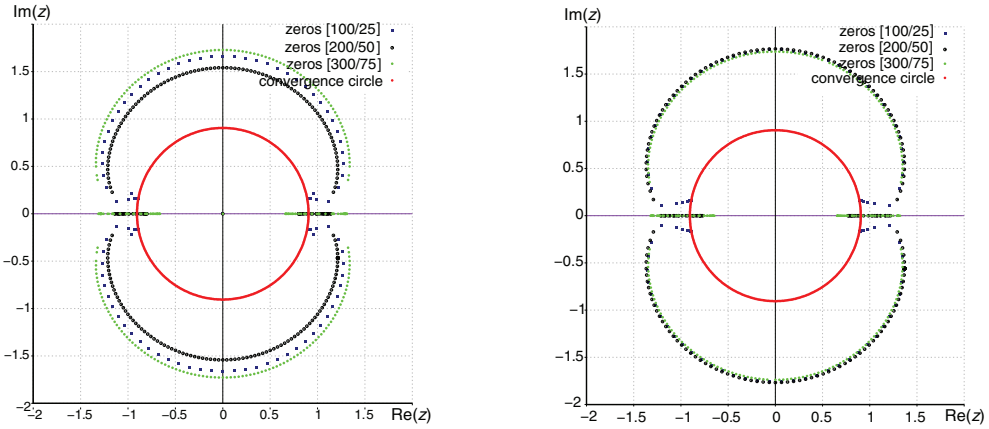

(*a*) (*b*)

Fig. 3. Distributions of zeros of PA $[4n/n]$ for $n = \{25, 50, 75\}$ to (*a*) the inverse Langevin function $\mathcal{L}^{-1}(x)$ and (*b*) modified one $f(x) = \dfrac{1-x^2}{3x}\mathcal{L}^{-1}(x)$ at $\zeta = 0$.

3. Zeros and poles of PAs to $\ln(1-z)$ and $-\dfrac{\ln(1-z)}{z}$. The first function studied in [2] is related to the Stieltjes function

$$f(z) = \int_0^1 \frac{dx}{1-xz} = -\frac{1}{z}\ln(1-z)$$

defined in the cut-plane $\mathbb{C} \setminus [1, \infty[$. The zeros and poles of PA defined by a power series of f expanded at the real points interlace on the cut $[1, \infty[$. One can question what happens if PA is defined at the complex point ζ? Klarsfeld remarked [7] that the Chisholm result [2] is wrong and showed that only the poles of PA to $\ln(1-z)$ follow the cut $\zeta + t(1-\zeta)$, $t \geq 1$, as mentioned in Introduction, but not the zeros. This result was generalized in [6] to all $m \geq n$. For the convenience let us introduce the following simplified notation for the cut:

$$\zeta + t(R-\zeta), \quad t \geq 1, \qquad [R, \infty[(\zeta)$$

directed by the straight line joining the point of development of $f : z = \zeta$ with the branch point $z = R$. Let us consider the following power expansions:

if $\zeta = 0$, then

$$f(z) = \ln(1-z) = \sum_{n=0}^{\infty} c_n z^n = -\sum_{n=1}^{\infty} \frac{1}{n} z^n,$$

if $\zeta \neq 0$, then

$$f(z) = \ln(1-\zeta) + \ln\left(1 - \frac{z-\zeta}{1-\zeta}\right) = \sum_{n=0}^{\infty} c_n^*(z-\zeta)^n = \ln(1-\zeta) - \sum_{n=1}^{\infty} \frac{1}{n}\left(\frac{z-\zeta}{1-\zeta}\right)^n, \quad (4)$$

where

$$c_0^* = \ln(1-\zeta), \quad c_n^* = \frac{c_n}{(1-\zeta)^n}, \quad n \geq 1.$$

Theorem 3.1 [6]. *Let $[m/n]$ and $[m/n]^*, m \geq n$, be the PAs of the function $f(z) = \ln(1-z)$ developed at the points $z = 0$ and $z = \zeta$, respectively. If z_k, $k = 1, 2, \ldots, n$, denotes a pole of $[m/n]$, then*

$$z_k^* = \zeta + z_k(1-\zeta)$$

denotes the pole of $[m/n]^*$. In other words, the poles of $[m/n]^*$ locate on the cut

$$[1, \infty[(\zeta), \zeta + t(1-\zeta), \quad t \geq 1. \quad (5)$$

The zeros of $[m/n]^*$ locate out of this line.

One can observe that the form (4) is particular for the function ln. Other Stieltjes functions do not follow this rule, i.e., if $f(z) = \sum a_n z^n$, then $f(z) \neq f(\zeta) + \sum a_n \left(\frac{z-\zeta}{1-\zeta}\right)^n$ for $\zeta \neq 0$.

(i) *Zeros and poles of PA $[n-1/n]$ and $[n/n]$ to $\ln(1-z)$.* This function has an exceptional property which leads to the Theorem 3.1 giving the location of poles. As shown in Fig. 4 the zeros are located left of the straight line of poles, approximately in the vicinity of an oblique straight line, except one zero. In the case $m \geq n$, Fig. 4 (*b*) and (*c*), the poles lie on the line joining the point of development of $f : z = \zeta$ with the branch point $z = 1$. When $m < n$, Fig. 4 (*a*), the poles deviate slightly from that line, except one pole (in this example $z_8 = 101.244 + 309.316i$), which is located quite distant from the mentioned line.

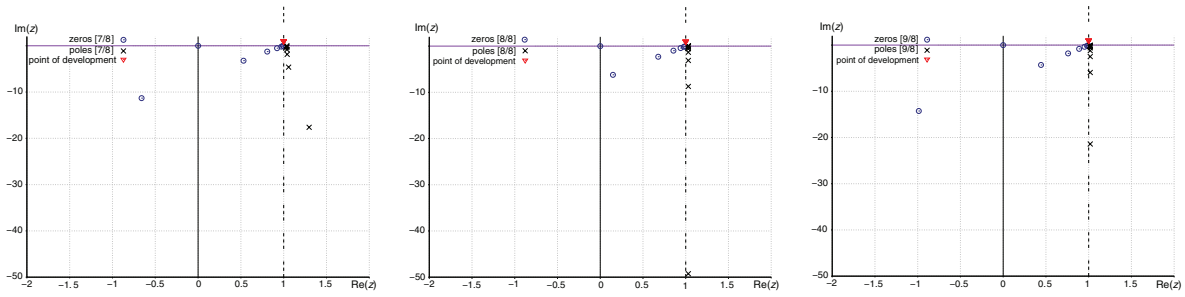

(*a*) (*b*) (*c*)

Fig. 4. Distributions of zeros and poles of (*a*) PA $[n-1/n]$, (*b*) PA $[n/n]$ and (*c*) PA $[n+1/n]$ to $\ln(1-z)$ at $\zeta = 1+i$ for $n = 8$. Each line connects the point of development of $f : z = \zeta$ with the branch point $z = 1$.

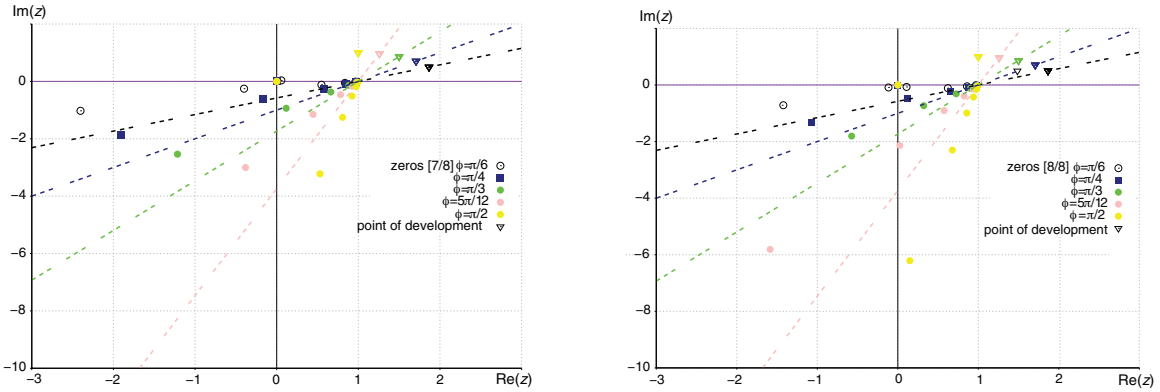

(*a*) (*b*)

Fig. 5. Distributions of zeros of (*a*) PA $[n-1/n]$ and (*b*) PA $[n/n]$ to $\ln(1-z)$ at $\zeta = 1 + e^{i\phi}$ for $n = 8$ and $\phi = \{\pi/6, \pi/4, \pi/3, 5\pi/12, \pi/2\}$. Each line connects the point of development of $f : z = \zeta$ with the branch point $z = 1$.

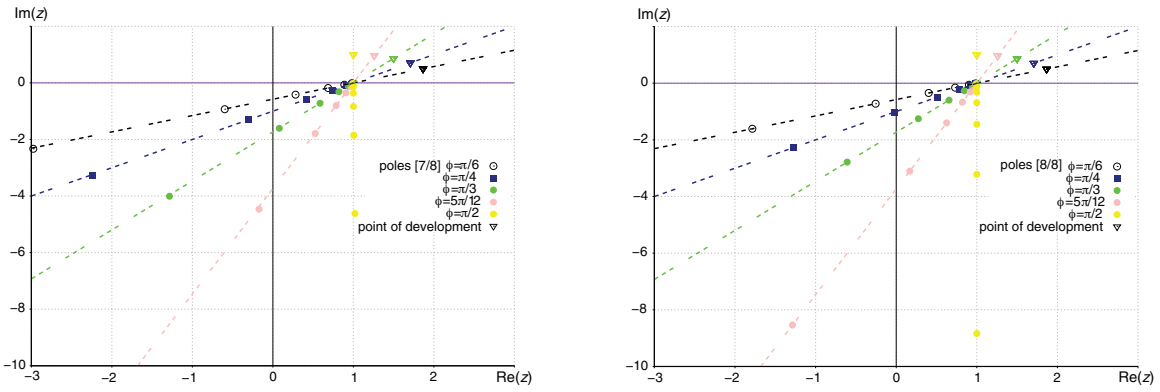

(*a*) (*b*)

Fig. 6. Distributions of poles of (*a*) PA $[n-1/n]$ and (*b*) PA $[n/n]$ to $\ln(1-z)$ at $\zeta = 1 + e^{i\phi}$ for $n = 8$ and $\phi = \{\pi/6, \pi/4, \pi/3, 5\pi/12, \pi/2\}$. Each line connects the point of development of $f : z = \zeta$ with the branch point $z = 1$.

This problem was further examined in more detail and included the following cases: a few equidistant points on the circle of radius 1 around the ramification point, namely $\zeta = 1 + e^{i\phi}$ and $\phi = \{\pi/6, \pi/4, \pi/3, 5\pi/12, \pi/2\}$, and on the other circle $\zeta = 1 + i + e^{i\phi}$ and the same set of ϕ as previous, to analyse the evolution of the location of zeros. The first case is illustrated in Figs. 5 (zeros) and 6 (poles). Figs. 7 (zeros) and 8 (poles) present the second case for the other circle. The figures mentioned before confirm the same behavior of the location of zeros and poles as in Fig. 4. In all cases for $[n-1/n]$ one zero lies near $z = 0$ and other locate on the straight line which is rotated by a certain angle with reference to a line which connects the point of development of $f : z = \zeta$ with the branch point $z = 1$. From Fig. 7 one can conclude that this angle is about $\pi/12$ for those points of development presented in this graph. All poles for $[n/n]$ lie on the straight line which connects the point of development of $f : z = \zeta$ with the branch point $z = 1$. Almost all poles for $[n-1/n]$ lie near the straight line which connects the point of development of $f : z = \zeta$ with the branch point $z = 1$, without one pole which locates quite distant from this line.

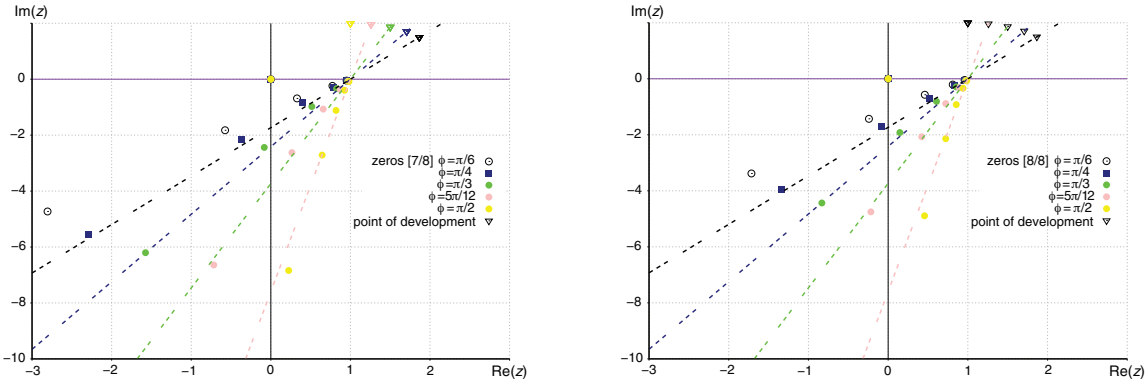

(*a*) (*b*)

Fig. 7. Distributions of zeros of (*a*) PA $[n-1/n]$ and (*b*) PA $[n/n]$ to $\ln(1-z)$ at $\zeta = 1+i+e^{i\phi}$ for $n=8$ and $\phi = \{\pi/6, \pi/4, \pi/3, 5\pi/12, \pi/2\}$. Each line connects the point of development of $f: z=\zeta$ with the branch point $z=1$.

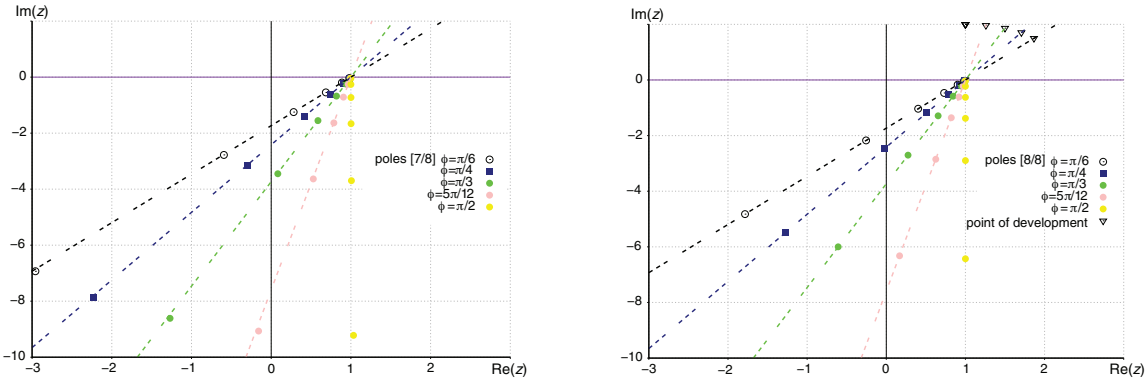

(*a*) (*b*)

Fig. 8. Distributions of poles of (*a*) PA $[n-1/n]$ and (*b*) PA $[n/n]$ to $\ln(1-z)$ at $\zeta = 1+i+e^{i\phi}$ for $n=8$ and $\phi = \{\pi/6, \pi/4, \pi/3, 5\pi/12, \pi/2\}$. Each line connects the point of development of $f: z=\zeta$ with the branch point $z=1$.

(ii) ***Several progressive deviations from*** $[1,\infty[(\zeta)$ ***lines of zeros and poles of PA to*** $-\dfrac{1}{z}\ln(1-z)$**.** The zeros of diagonal and subdiagonal PA to $f(z) = -\dfrac{1}{z}\ln(1-z)$ computed at $\zeta = 0$ interlace on the cut $[1,\infty[(0)$ (Fig. 9).

The zeros of diagonal and subdiagonal PA to f computed at the points $0.2i, \ldots, 10i$ locate on the under sides of $[1,\infty[(\zeta)$ consecutive lines (or cuts). The poles of $[n/n]$ and $[n-1/n]$ $(n \le 8)$ locate on the upper sides of these lines. The moving zeros and poles deviate more and more from $[1,\infty[(\zeta)$ with $|\zeta|$ forming the shape of the form $\wedge$. When $|\zeta| \to 0$ one receives the distribution of poles and zeros, which is demonstrated in Fig. 9. From Fig. 10 one concludes that for small $|\zeta|$ such as two the zeros and poles of diagonal and subdiagonal PA to f locate on $[1,\infty[(\zeta)$ line.

The location of the zeros of $[m/n]^*$ remains an open problem. However, the following remarks can maybe unlock this question. The particular case of a theorem given in [2, p. 217] says that if $[n/n]_f$ is a PA of some function f and α a constant, then

$$[n/n]_f + \alpha = [n/n]_{f+\alpha}.$$

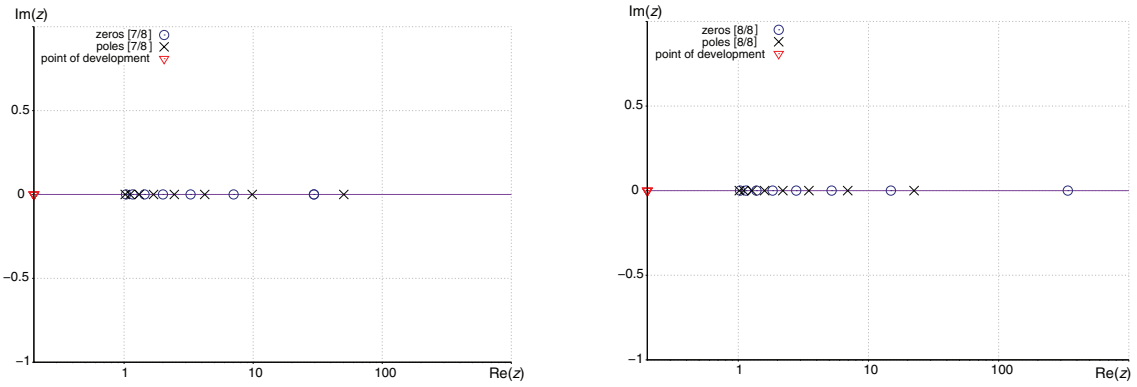

(*a*) (*b*)

Fig. 9. Distributions of zeros and poles of (*a*) PA $[n-1/n]$ and (*b*) PA $[n/n]$ to $f(z) = -\frac{1}{z}\ln(1-z)$ at $\zeta = 0$ for $n = 8$ which are plotted on a semi logarithmic scale. They interlace on the cut $[1, \infty[(0)$.

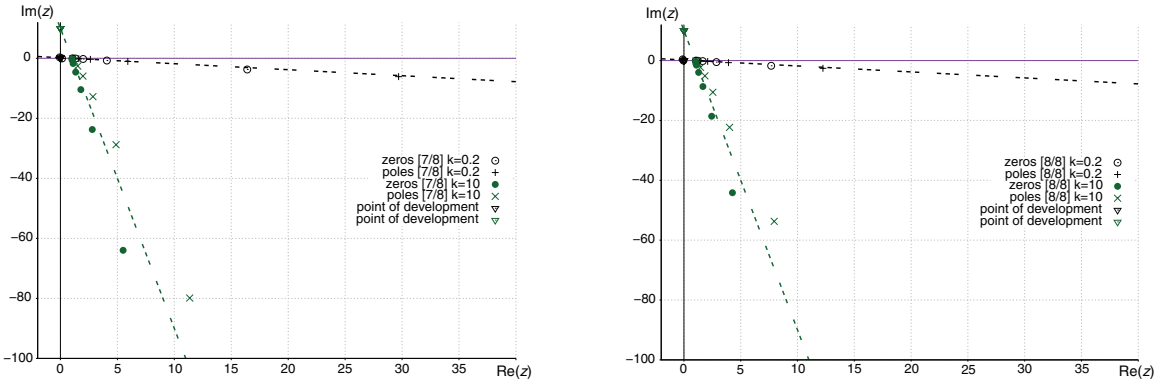

(*a*) (*b*)

Fig. 10. Distributions of zeros and poles of (*a*) PA $[n-1/n]$ and (*b*) PA $[n/n]$ to $-\frac{1}{z}\ln(1-z)$ at $\zeta = ki$ for $k = \{0.2, 10\}$ and $n = 8$. Each line connects the point of development of $f : z = \zeta$ with the branch point $z = 1$.

It readily leads to the following theorem, where all notations are the same as in Theorem 3.1 except c_0^* which is replaced by an arbitrary constant α.

Theorem 3.2. *Let* $g(z) = \ln(1-z) - \ln(1-\zeta) = \ln\left(\dfrac{1-z}{1-\zeta}\right)$, *then*

$$[n/n]_g(z) = \frac{P_n\left(\dfrac{z-\zeta}{1-\zeta}\right)}{Q_n\left(\dfrac{z-\zeta}{1-\zeta}\right)} = \frac{p_0 + p_1\left(\dfrac{z-\zeta}{1-\zeta}\right) + \ldots + p_n\left(\dfrac{z-\zeta}{1-\zeta}\right)^n}{1 + q_1\left(\dfrac{z-\zeta}{1-\zeta}\right) + \ldots + q_n\left(\dfrac{z-\zeta}{1-\zeta}\right)^n}$$

and all zeros and poles of this PA interlace on the cut $[1, \infty[(\zeta)$ (5). *If* $\alpha \neq 0$, *then*

$$[n/n]_{g+\alpha}(z) = [n/n]_g(z) + \alpha = \frac{\alpha Q_n\left(\dfrac{z-\zeta}{1-\zeta}\right) + P_n\left(\dfrac{z-\zeta}{1-\zeta}\right)}{Q_n\left(\dfrac{z-\zeta}{1-\zeta}\right)} = \frac{P_n^*\left(\dfrac{z-\zeta}{1-\zeta}\right)}{Q_n^*\left(\dfrac{z-\zeta}{1-\zeta}\right)}.$$

If $\alpha = 0$, then the poles and also the zeros simulate the cut $[1, \infty[(\zeta)$. The problem consists in analyzing the behavior of the zeros of P_n^* as function of complex α, in particular with $\alpha = c_0^* = \ln(1-\zeta)$ and, if possible, to bound the position of all zeros. One observes that the zeros of PA of $\ln(1-z)$ correspond to the zeros of $P_n^* = \ln(1-\zeta)Q_n\left(\dfrac{z-\zeta}{1-\zeta}\right) + P_n\left(\dfrac{z-\zeta}{1-\zeta}\right)$.

4. Zeros and poles of PAs at complex and complex conjugate points. In this section $[m/n]_f(z-\zeta)$ and $[m/n]_f^*(z-\overline{\zeta})$ denote the PAs of a complex-symmetric function f at the point ζ and its complex conjugate $\overline{\zeta}$, respectively.

Theorem 4.1. *Let* $[m/n] = \dfrac{P_m}{Q_n}$ *and* $[m/n]^* = \dfrac{P_m^*}{Q_n^*}$ *be PAs of a complex-symmetric function* f *at* ζ *and* $\overline{\zeta}$. *Then the zeros and the poles of* $[m/n]$ *are complex conjugate of the corresponding zeros and poles of* $[m/n]^*$.

Proof. Eq. (3) gives

$$f(z) = \sum_{i=0}^{\infty} c_i(z-\zeta)^i = \sum_{i=0}^{\infty} \overline{c_i}(z-\overline{\zeta})^i, \tag{6}$$

$Q_n = 1 + q_1(z-\zeta) + \ldots + q_n(z-\zeta)^n$ and, due to (6), $Q_n^* = 1 + \overline{q_1}(z-\overline{\zeta}) + \ldots + \overline{q_n}(z-\overline{\zeta})^n$. Then the zeros of Q_n^* are the complex conjugate of those of Q_n . The same arguments are used for P_m and P_m^* which completes the proof.

This fact is documented in Fig. 11.

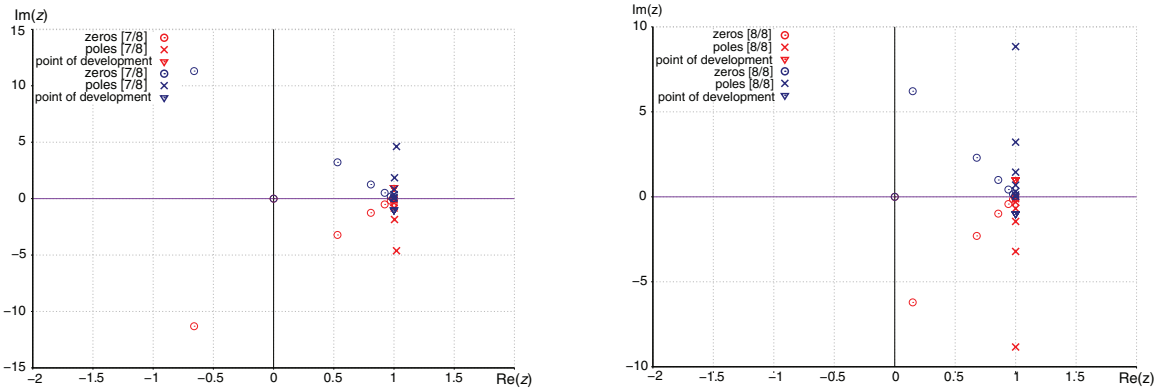

(*a*) (*b*)

Fig. 11. Distributions of zeros and poles of (*a*) PA $[n-1/n]$ and (*b*) PA $[n/n]$ to $\ln(1-z)$ at $\zeta = 1+i$ and $\overline{\zeta} = 1-i$ for $n = 8$. The zeros and the poles of $[m/n]$ are complex conjugate of the corresponding zeros and poles of $[m/n]^*$.

5. NPAs of the complex-symmetric functions. The following theorem is the consequence of Theorem 3.1.

Theorem 5.1 [6]. *Let* f *be a complex-symmetric function, then the zeros and poles of* 2*-point PA* $[m/n]_{\zeta\overline{\zeta}}^{ll'}$ *of* f *are complex conjugate of the zeros and poles of* $[m/n]_{\zeta\overline{\zeta}}^{l'l}$, *where* l *and* l' *are the arbitrary integers satisfying the condition* $l + l' = m + n + 1$.

Fig. 12 illustrates the Theorem 5.1. It includes 3 cases of different distribution of pieces of information. We observe that when the amount of information approaching the symmetrical form

then zeros and poles tend to the real axis. Fig. 12 (*c*) shows the situation when the symmetric state is achieved. Then we observe that all zeros and poles interlace on the real cut $[1, \infty[(0)$.

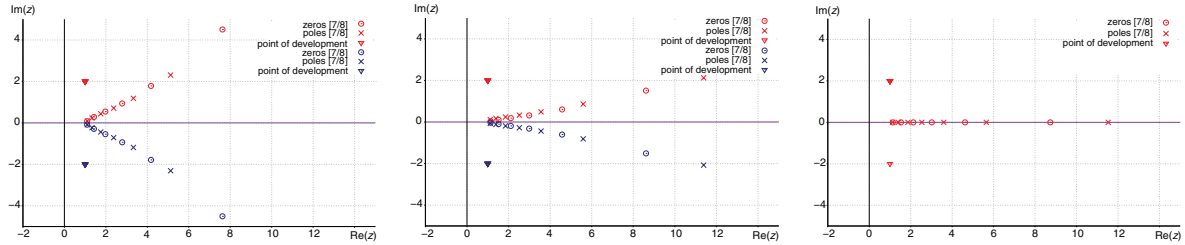

(*a*) (*b*) (*c*)

Fig. 12. Distributions of zeros and poles of (*a*) $[7/8]^{5\ 11}_{1+2i,1-2i}$ (rising branch) and $[7/8]^{11\ 5}_{1+2i\ 1-2i}$ NPA, (*b*) $[7/8]^{7\ 9}_{1+2i\ 1-2i}$ and $[7/8]^{9\ 7}_{1+2i\ 1-2i}$, (*c*) $[7/8]^{8\ 8}_{1+2i\ 1-2i}$ to $-\dfrac{1}{z}\ln(1-z)$.

Fig. 13 shows distributions of zeros and poles for two different development points (a) $\zeta = = 1 + 0.2i$ and (b) $\zeta = 1 + i$. They have the similar distribution as previous ones.

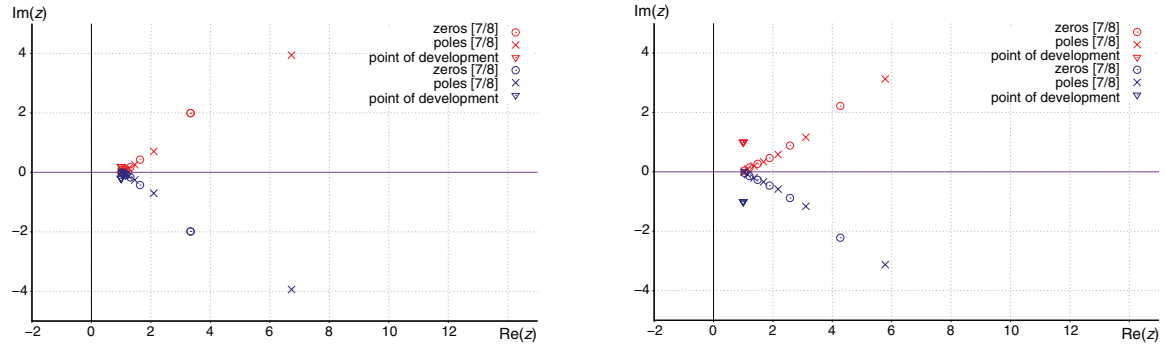

(*a*) (*b*)

Fig. 13. Distributions of zeros and poles of (*a*) $[7/8]^{5\ 11}_{1+0.2i,1-0.2i}$ (rising branch) and $[7/8]^{11\ 5}_{1+0.2i\ 1-0.2i}$ NPA, (*b*) $[7/8]^{5\ 11}_{1+i\ 1-i}$ and $[7/8]^{11\ 5}_{1+i\ 1-i}$ to $-\dfrac{1}{z}\ln(1-z)$.

***Corollary* 5.1** [6]. *Let f be a complex-symmetric function. Then the zeros and poles of NPA $[m/n]^{l_1\ldots l_k l'_1\ldots l'_k}_{\zeta_1\ldots\zeta_k\overline{\zeta_1}\ldots\overline{\zeta_k}}$ complex conjugate of the zeros and poles of $[m/n]^{l_1\ldots l_k l'_1\ldots l'_k}_{\zeta_1\ldots\zeta_k\overline{\zeta_1}\ldots\overline{\zeta_k}}$, where $l_1 + +l_2 + \ldots + l_k + l'_1 + l'_2 + \ldots + l'_k = m + n + 1$.*

Theorem 5.2 [6]. *Let f be a complex-symmetric function. Then all coefficients of NPA $[m/n]^{l_1\ldots l_k l_1\ldots l_k}_{\zeta_1\ldots\zeta_k\overline{\zeta_1}\ldots\overline{\zeta_k}}$ of f, where $2(l_1 + l_2 + \ldots + l_k) = m + n + 1$, are real.*

We performed numerous numerical computations whose results lead to the following theorem.

Theorem 5.3. *Let f be a complex-symmetric function. Then all the zeros and poles of NPAs $[n-1/n]^{l_1\ldots l_k l_1\ldots l_k}_{\zeta_1\ldots\zeta_k\overline{\zeta_1}\ldots\overline{\zeta_k}}$ and $[n/n-1]^{l_1\ldots l_k l_1\ldots l_k}_{\zeta_1\ldots\zeta_k\overline{\zeta_1}\ldots\overline{\zeta_k}}$ of f, where $2(l_1 + l_2 + \ldots + l_k) = m + n + 1$, are real and interlace on the cut of the function.*

The general proof of this theorem remains an open problem. We are convinced that the only candidates between NPAs, whose all the zeros and poles are real, belong to approximants with real coefficients. It means that they must satisfy Theorem 5.2. We proved it in the simplest form NPAs [1/2] and [2/1], which is presented in the next example. As shown despite the apparent simplicity of

the chosen approximants, one gets very complicated mathematical formulas on the coefficients and then poles and zeros.

Theorem 5.3 is illustrated numerically in Table 1. Only NPAs [3/4] and [4/3] have all the zeros and poles real. Table 2 confirms that all NPAs from Table 1 have real coefficients.

Table 1. Distributions of zeros and poles of NPA $[m/n]^{4}_{1+2i,1-2i}$ to $-\dfrac{1}{z}\ln(1-z)$

[1/6]		[2/5]		[3/4]	
zeros	poles	zeros	poles	zeros	poles
1.92359	$-4.10447 + 4.57707i$	1.61757	$-7.07786 - 20.2624i$	1.52964	1.22367
	$-4.10447 - 4.57707i$	3.46555	$-7.07786 + 20.2624i$	3.03277	2.11415
	1.36082		1.25579	8.96214	4.18872
	2.8988		2.27595		16.0223
	$3.4331 + 5.92542i$		5.09943		
	$3.4331 - 5.92542i$				

[4/3]		[5/2]		[6/1]	
zeros	poles	zeros	poles	zeros	poles
-35.5846	1.2437	-7.9627	1.3174	-2.4522	1.5287
1.5843	2.2143	$0.5564 + 8.9102i$	2.6162	$-0.7666 - 4.0899i$	
3.2911	4.7095	$0.5564 - 8.9102i$		$-0.7666 + 4.0899i$	
15.1603		1.793		2.5359	
		4.8891		$2.758 - 3.8783i$	
				$2.758 + 3.8783i$	

Table 2. NPA $[m/n]^{4}_{1+2i,1-2i}$ to $-\dfrac{1}{z}\ln(1-z)$

$$[1/6] = \frac{0.9795 - 0.5092z}{0.000143z^6 - 0.0004171z^5 + 0.003797z^4 + 0.001442z^3 + 0.193z^2 - 1.009z + 1}$$

$$[2/5] = \frac{0.1775z^2 - 0.9026z + 0.9954}{-0.0001489z^5 - 0.0008228z^4 - 0.05352z^3 + 0.5503z^2 - 1.401z + 1}$$

$$[3/4] = \frac{-0.02399z^3 + 0.3245z^2 - 1.09252z + 0.9976}{0.005759z^4 - 0.1356z^3 + 0.7899z^2 - 1.5913z + 1}$$

$$[4/3] = \frac{-0.0003542z^4 - 0.005507z^3 + 0.2245z^2 - 0.9694z + 0.9964}{-0.07709z^3 + 0.6297z^2 - 1.4679z + 1}$$

$$[5/2] = \frac{0.0001775z^5 + 0.00002975z^4 + 0.006z^3 + 0.03929z^2 - 0.6427z + 0.9878}{0.2901z^2 - 1.1412z + 1}$$

$$[6/1] = \frac{-0.000377z^6 + 0.001533z^5 - 0.009659z^4 + 0.01457z^3 - 0.07590z^2 - 0.1301z + 0.9194}{1 - 0.6541z}$$

Example of analytical solution of distribution of zeros and poles of NPAs $\boldsymbol{[1/2]^{\mathbf{2}\,\mathbf{2}}_{\zeta,\bar{\zeta}}}$ ***and*** $\boldsymbol{[2/1]^{\mathbf{2}\,\mathbf{2}}_{\zeta,\bar{\zeta}}}$ ***to*** $\boldsymbol{-\dfrac{1}{z}\ln(1-z)}$**.** Next we find exact solutions for the locations of zeros and poles in the case of NPA $[1/2]^{22}_{\zeta\bar{\zeta}}(z)$ to the Stieltjes function $f(z) = -\dfrac{\ln(1-z)}{z}$. The problem can be expressed as follows:

$$[1/2]^{22}_{\zeta\bar{\zeta}}(z) = \frac{a_0 + a_1 z}{1 + b_1 z + b_2 z^2}.$$

The Taylor series expansion to the Stieltjes function f developed in the arbitrary point ζ is given by the formula

$$f(z) = -\frac{\ln(1-z)}{z} = c_0 + c_1(z-\zeta) + O\left((z-\zeta)^2\right). \tag{7}$$

Theorem 5.4. *Let* $f(z) = -\dfrac{\ln(1-z)}{z}$ *and* $c_n(z)$ *be coefficients of the the Taylor series expansion to the Stieltjes function* $f(z)$*. Then*

$$c_n(z) = \frac{n!(-1)^{n-1}\ln(1-z)}{z^{n+1}} + \sum_{k=1}^{n} \frac{(-1)^{n-k}n!}{k(1-z)^k z^{n-k+1}}.$$

Proof. We use the general Leibniz rule which states that if f and g are n-times differentiable functions, then the product fg is also n-times differentiable and its nth derivative is given by

$$(fg)^{(n)}(x) = \sum_{k=0}^{n} \binom{n}{k} f^{(n-k)}g^{(k)}(x) = \sum_{k=1}^{n} \binom{n}{k} f^{(n-k)}g^{(k)}(x) + n!f^{(n)}g^{(0)}(x),$$

where $\binom{n}{k} = \dfrac{n!}{k!(n-k)!}$ is the binomial coefficient and $f^{(0)}(x) = f(x)$, $g^{(0)}(x) = g(x)$.

The following formulas for the nth derivatives of both functions $f(x) = x^{-1}$ and $g(x) = -\ln(1-x)$ are valid

$$f^{(n)}(x) = (-1)^n n! x^{-n-1},$$

$$g^{(n)}(x) = (n-1)!(1-x)^{-n}, \quad n \geq 1,$$

$$g^{(0)}(x) = -\ln(1-x).$$

Using the general Leibniz rule and mentioned before formulas for the nth derivatives of functions f and g, we get a general formula for the nth derivative of Stieltjes function $-\dfrac{\ln(1-z)}{z}$:

$$\left(-\frac{\ln(1-x)}{x}\right)^{(n)}(x) = (fg)^{(n)}(x) =$$

$$= n!(-1)^n x^{-n-1}(-\ln(1-x)) + \sum_{k=1}^{n} \binom{n}{k}(k-1)!(-1)^{n-k}(n-k)!x^{k-n-1}(1-x)^{-k} =$$

$$= \frac{n!(-1)^{n-1}\ln(1-x)}{x^{n+1}} + \sum_{k=1}^{n} \frac{(-1)^{n-k}n!}{k(1-x)^k x^{n-k+1}}.$$

Using Theorem 5.4, one can readily obtain $c_0 = -\dfrac{\ln(1-\zeta)}{\zeta}$ and $c_1 = \dfrac{1}{\zeta}\left(\dfrac{1}{1-\zeta} - \dfrac{\ln(1-\zeta)}{\zeta}\right)$, which should be inserted in Eq. (7). Then the problem of 2-point Padé to $f(z)$ (Eq. (7)) can be formulate by the use of the following matrix representation of the linear system for unknown coefficients $a_0,\ a_1,\ b_1,\ b_2$:

$$\begin{bmatrix} 1 & \zeta & -c_0\zeta & -c_0\zeta^2 \\ 1 & \overline{\zeta} & \overline{-c_0\zeta} & \overline{-c_0\zeta^2} \\ 0 & 1 & -c_0 - c_1\zeta & -2c_0\zeta - c_1\zeta^2 \\ 0 & 1 & \overline{-c_0 - c_1\zeta} & \overline{-2c_0\zeta - c_1\zeta^2} \end{bmatrix} \begin{bmatrix} a_0 \\ a_1 \\ b_1 \\ b_2 \end{bmatrix} = \begin{bmatrix} c_0 \\ \overline{c_0} \\ c_1 \\ \overline{c_1} \end{bmatrix}. \tag{8}$$

It can be expressed more conveniently for the further computation using the simple transformation of rows of the matrix such as adding or subtraction. For simplification one can use the formulas like $\zeta + \overline{\zeta} = 2\mathrm{Re}\,(\zeta)$, $\zeta - \overline{\zeta} = 2\,\mathrm{Im}\,(\zeta)$. Finally, we obtain the following matrix equation (Eq. (9)) whose elements are real. One can note that such a transformation can be performed for any matrix which results from Theorem 5.2. It is evident that unknown coefficients which are found from this equation must also be real. It leads to the fact that zero is always real (solution of the linear equation $a_0 + a_1 z = 0$) but the poles do not have to be real. This fact will be revisited after finding the coefficients b_1 and b_2:

$$\begin{bmatrix} 1 & \mathrm{Re}\,(\zeta) & -\mathrm{Re}\,(c_0\zeta) & -\mathrm{Re}\,(c_0\zeta^2) \\ 0 & \mathrm{Im}\,(\zeta) & -\mathrm{Im}\,(c_0\zeta) & -\mathrm{Im}\,(c_0\zeta^2) \\ 0 & 1 & -\mathrm{Re}\,(c_0 + c_1\zeta) & -\mathrm{Re}\,(2c_0\zeta + c_1\zeta^2) \\ 0 & 0 & -\mathrm{Im}\,(c_0 + c_1\zeta) & -\mathrm{Im}\,(2c_0\zeta + c_1\zeta^2) \end{bmatrix} \begin{bmatrix} a_0 \\ a_1 \\ b_1 \\ b_2 \end{bmatrix} = \begin{bmatrix} \mathrm{Re}\,(c_0) \\ \mathrm{Im}\,(c_0) \\ \mathrm{Re}\,(c_1) \\ \mathrm{Im}\,(c_1) \end{bmatrix}. \tag{9}$$

The general solution for unknown coefficients a_0, a_1, b_1, b_2 is given in Appendix A. We provide the exact formulas for zero and poles. Because they are very complicated, we also present the solution for the particular case of $\zeta = 1 + iy$, whose behavior can reflect the general situation. It is easier to analyse the distribution of the zero and poles in the two-dimensional case than spatial (3D) one. To summarize the obtained results, we show them below in the form of graphs (Fig. 14). They clearly illustrate the fact that poles are real and interlace the zero on the real cut $[1, \infty[(0)$.

The same procedure was applied to NPA $[2/1]^{2\,2}_{\zeta,\overline{\zeta}}$. For simplicity, we only provide a solution in the form of graphs. Fig. 15 confirms that all the zeros and poles are real and interlace on the real axis.

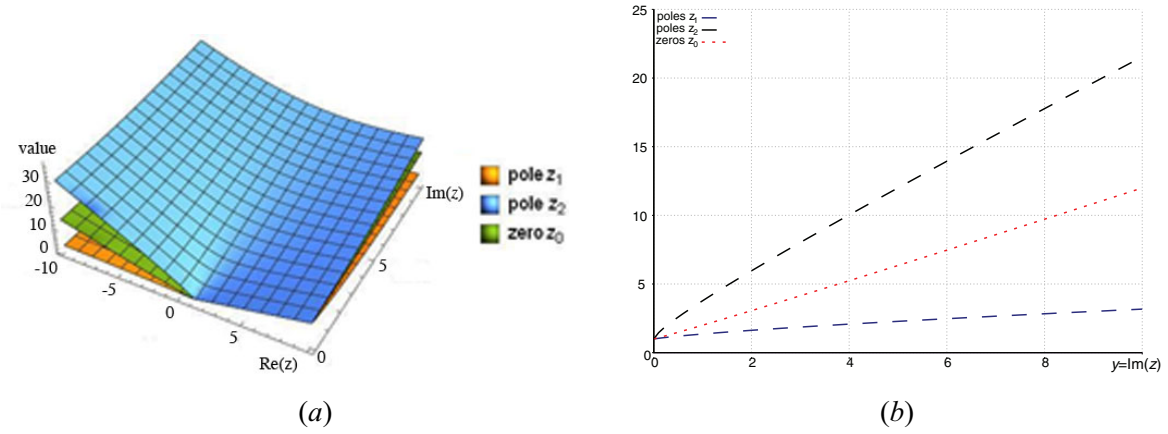

(*a*) (*b*)

Fig. 14. Distribution of zeros and poles for (*a*) spatial case $[1/2]^{2}_{x+yi,x-yi}$ NPA to $-\dfrac{1}{z}\ln(1-z)$, (*b*) two-dimensional case $[1/2]^{2}_{1+yi,1-yi}$ NPA for continuous values of $y = \mathrm{Im}\,(z)$.

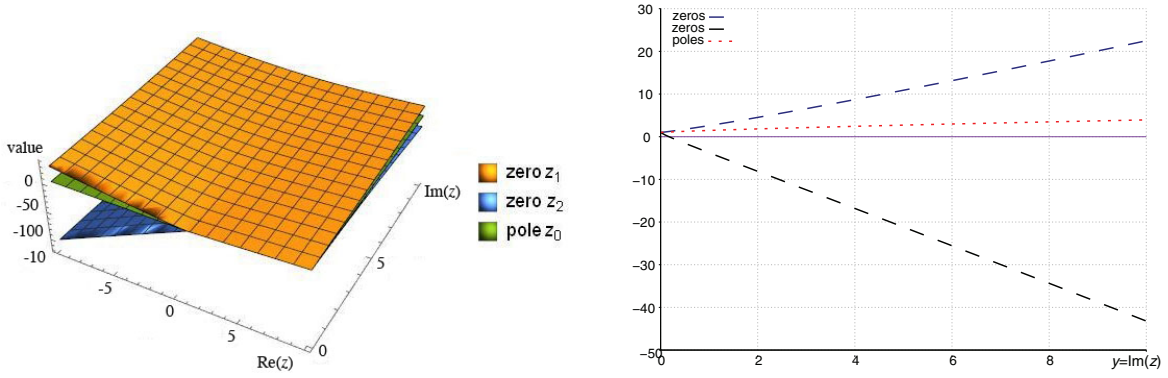

(*a*) (*b*)

Fig. 15. Distribution of zeros and poles for (*a*) spatial case $[2/1]^{2}_{x+yi,x-yi}$ NPA to $-\frac{1}{z}\ln(1-z)$, (*b*) two-dimensional case $[2/1]^{2}_{1+yi,1-yi}$ NPA for continuous values of $y = \mathrm{Im}(z)$.

6. Characteristic location of zeros and poles and convergence of PA: numerical observations. To appreciate the speed of convergence of diagonal PA $[n/n]$ to Sieltjes functions f in different directions starting from the point ζ of development of f one analyze [8] the so-called equierror curves which border the regions defined by

$$D_\varepsilon = z : |f(z) - [n/n]_\zeta(z)| \le \varepsilon$$

for different ε. It was remarked that for the points ζ equidistant with respect to the ramification point R (here $R = 1$) the convergence is a little better for ζ real. More, the convergence is, in general, better going from R to ∞, and worse in the opposite direction from ζ to R. The non-rational Stieltjes functions f defined by (2) in a complex cut plane have no zeros and no poles. The zeros and poles of diagonal and subdiagonal PA to f defined at $z = 0$ localize the cut on $[R, \infty[$. If the point of development ζ is complex, the cut can be $z(t) = \zeta + t(R - \zeta), t \ge 1$; in the following we note this line $[R, \infty[(\zeta)$. If we observe the concentration of poles and zeros of PA at the vicinity of some lines as $[R, \infty[$, we have a natural tendency to interpret this as a localization of the cut. However an essential problem of approximation concerns the domain of convergence, and the convergence of PA to Stieltjes functions depends on the position of poles and zeros, the choice of the cut being secondary. Observing the following numerical results, we remark specific order, the proximity of zeros and (or) poles to certain lines. Visibly these localizations follow some rules. It is to be discovered. In this paper, we present the results relative to the function $\ln(1-z)$, to the Stieltjes function $-\dfrac{\ln(1-z)}{z}$ and to its inverted function. In fact, other Stieltjes functions as $\dfrac{\pi}{\sqrt{1-z^2}}$ or $\dfrac{\sqrt{1+z}-1}{z}$ present similar properties (Fig. 16).

(i) ***Exceeding zeros and poles of* 6*-point PA to*** $\boldsymbol{f(z) = -\dfrac{\ln(1-z)}{z}}$**.** The zeros of truncated Mclaurin series are located on the convergence circle (Fig. 17).

The two following figures (Fig. 18 (*a*), (*b*)) show that the exceeding zeros of [12/3], [22/3], [30/3] and the exceeding poles of [3/12], [3/22], [3/30], progress to the convergence circle. The six considered points of development are: $i, -i, 1+i, 1-i, -1+2i, -1-2i$.

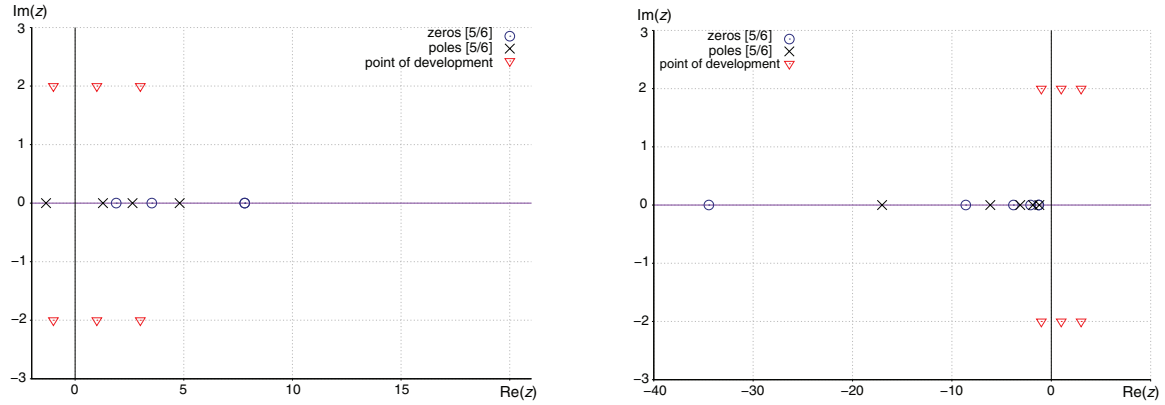

(*a*) (*b*)

Fig. 16. Distributions of zeros and poles of NPA $[5/6]^{2}_{1+2i}{}^{2}_{1-2i}{}^{2}_{-1+2i}{}^{2}_{-1-2i}{}^{2}_{3+2i}{}^{2}_{3-2i}$ to (*a*) $f(z) = \dfrac{\pi}{\sqrt{1-z^2}}$ and (*b*) $f(z) = \dfrac{\sqrt{z+1}-1}{z}$.

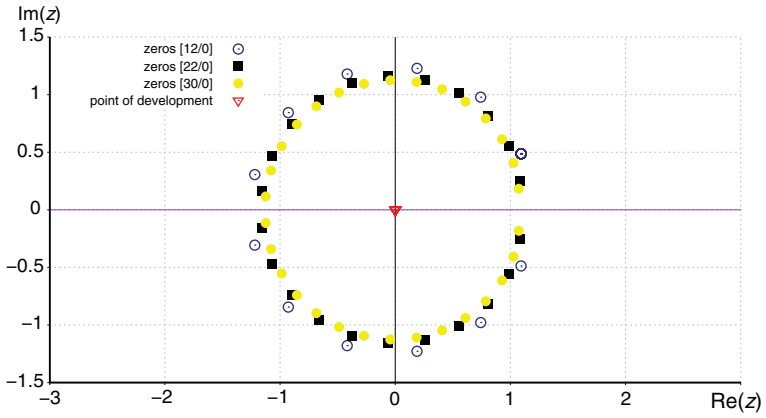

Fig. 17. Distributions of zeros of [12/0], [22/0], [30/0] PAs to $f(z) = -\dfrac{\ln(1-z)}{z}$ at $\zeta = 0$.

(ii) ***Power expansions at the symmetric points on the oblique line.*** Let us consider the development points on the line $D^{\theta}_{R} = \{z(t) = R + te^{i(\theta+\frac{\pi}{2})}; t \in \mathbb{R}\}$, symmetrical with respect to the ramification point R (Fig. 19).

We observed that the zeros and poles of PA to $-\dfrac{\ln(1-z)}{z}$ interlace approximatively on $D^{\theta}_{\perp R}$. That fact is documented in Fig. 20 for three different angles $\theta = \{\arctan(1/2), \arctan(1), \arctan(2)\}$. Figs. 21 and 22 confirm the similar behavior of the zeros and poles of PA for other combinations of development points and amount of information taken for PAs.

Unfortunately two poles of $[1/2]^{2}_{i}{}^{2}_{2-i}(z)$ deviate from this line (Fig. 23).

However, a remarkable regularity was observed: the real part of all zeros and poles located in the vicinity of $D^{\theta}_{\perp R}$ are almost equal to the zeros and poles located on the real axis (on $D^{0}_{\perp R}$) as shown in Fig. 24.

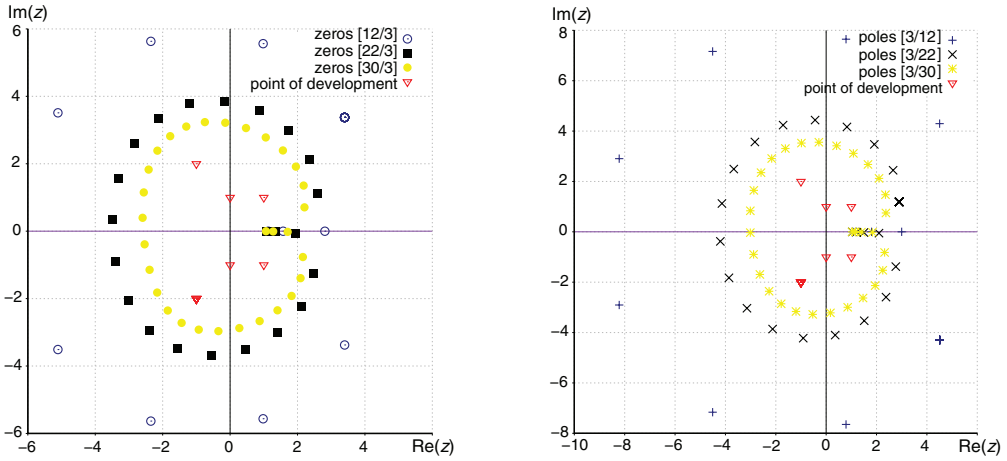

(*a*) (*b*)

Fig. 18. Distributions of (*a*) zeros exceeding of [12/3], [22/3], [30/3] NPAs and (*b*) exceeding poles of [3/12], [3/22], [3/30] to $f(z) = -\dfrac{\ln(1-z)}{z}$.

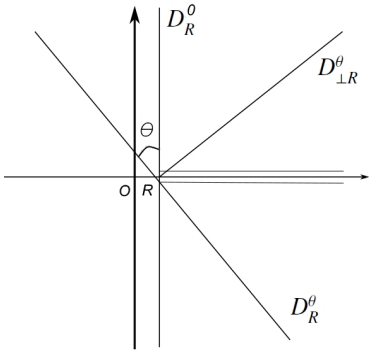

Fig. 19. D_R^{θ} and $D_{\perp R}^{\theta} \perp D_R^{\theta}$.

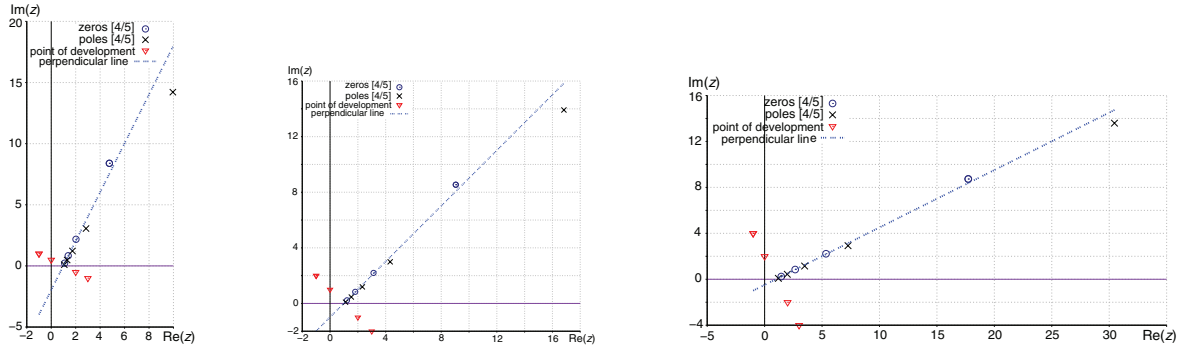

(*a*) (*b*) (*c*)

Fig. 20. Distributions of zeros and poles of $[4/5]^{2\ 2\ 2\ 2}_{z_1 z_2 z_3 z_4}$ NPA to $f(z) = -\dfrac{\ln(1-z)}{z}$: (*a*) $\theta = \arctan(1/2), z_1 = 1/2i,\ z_2 = 2 - 1/2i,\ z_3 = 3 - i,\ z_4 = -1 + i$, (*b*) $\theta = \arctan(1) = \pi/4,\ z_1 = i,\ z_2 = 2 - i,\ z_3 = 3 - 2i,\ z_4 = -1 + 2i$, (*c*) $\theta = \arctan(2),\ z_1 = 2i,\ z_2 = 2 - 2i,\ z_3 = 3 - 4i,\ z_4 = -1 + 4i$.

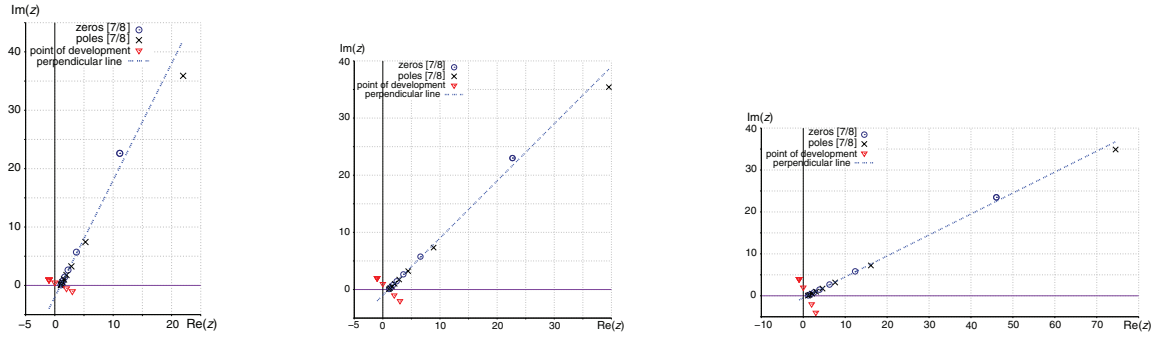

(*a*) (*b*) (*c*)

Fig. 21. Distributions of zeros and poles of $[7/8]^{4\ 4\ 4\ 4}_{z_1 z_2 z_3 z_4}$ NPA to $f(z) = -\dfrac{\ln(1-z)}{z}$: (*a*) $\theta = \arctan(1/2), z_1 = 1/2i,\ z_2 = 2 - 1/2i,\ z_3 = 3 - i,\ z_4 = -1 + i$, (*b*) $\theta = \arctan(1) = \pi/4,\ z_1 = i,\ z_2 = 2 - i,\ z_3 = 3 - 2i,\ z_4 = -1 + 2i$, (*c*) $\theta = \arctan(2),\ z_1 = 2i,\ z_2 = 2 - 2i,\ z_3 = 3 - 4i,\ z_4 = -1 + 4i$.

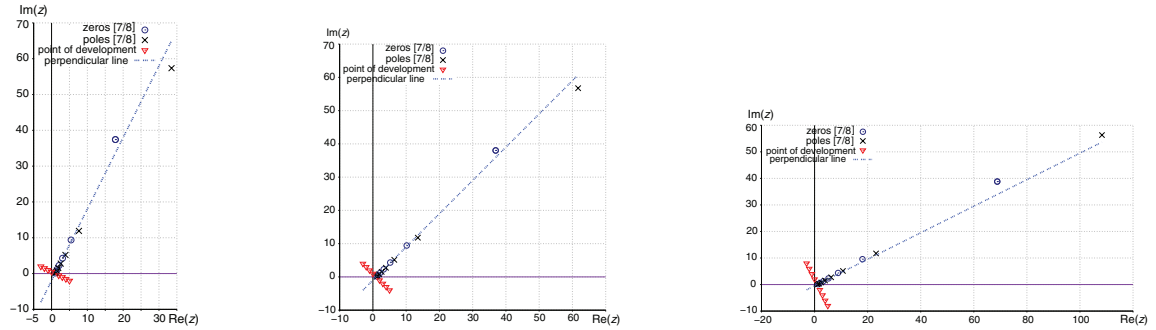

(*a*) (*b*) (*c*)

Fig. 22. Distributions of zeros and poles of $[7/8]^{2\ 2\ 2\ 2\ 2\ 2\ 2\ 2}_{z_1 z_2 z_3 z_4 z_5 z_6 z_7 z_8}$ NPA to $f(z) = -\dfrac{\ln(1-z)}{z}$: (*a*) $\theta = \arctan(1/2),\ z_1 = 1/2i,\ z_2 = 2 - 1/2i,\ z_3 = 3 - i,\ z_4 = -1 + i,\ z_5 = 4 - 3/2i,\ z_6 = -2 + 3/2i,\ z_7 = 5 - 2i,\ z_8 = -3 + 2i$, (*b*) $\theta = \arctan(1) = \pi/4,\ z_1 = i,\ z_2 = 2 - i,\ z_3 = 3 - 2i,\ z_4 = -1 + 2i,\ z_5 = 4 - 3i,\ z_6 = -2 + 3i,\ z_7 = 5 - 4i,\ z_8 = -3 + 4i$, (*c*) $\theta = \arctan(2),\ z_1 = 2i,\ z_2 = 2 - 2i,\ z_3 = 3 - 4i,\ z_4 = -1 + 4i,\ z_5 = 4 - 6i,\ z_6 = -2 + 6i,\ z_7 = 5 - 8i,\ z_8 = -3 + 8i$.

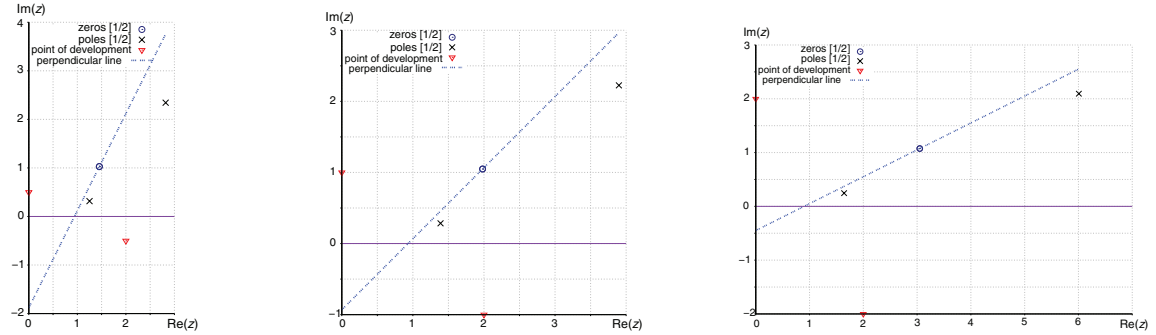

(*a*) (*b*) (*c*)

Fig. 23. Distributions of zeros and poles of $[1/2]^{2\ 2}_{z_1 z_2}$ NPA to $f(z) = -\dfrac{\ln(1-z)}{z}$: (*a*) $\theta = \arctan(1/2),\ z_1 = 1/2i,\ z_2 = 2 - 1/2i$, (*b*) $\theta = \arctan(1) = \pi/4,\ z_1 = i,\ z_2 = 2 - i$, (*c*) $\theta = \arctan(2),\ z_1 = 2i,\ z_2 = 2 - 2i$.

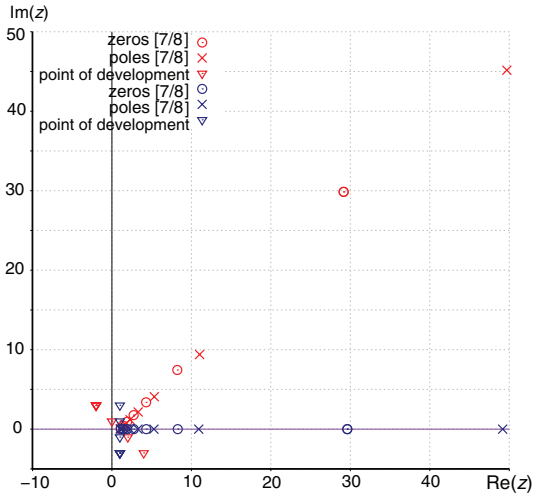

Fig. 24. Distributions of zeros and poles of $[7/8]^{4\ 4\ 4\ 4}_{z_1 z_2 z_3 z_4}$ NPA and $[7/8]^{4\ 4\ 4\ 4}_{z_1^* z_2^* z_3^* z_4^*}$ to $f(z) = -\dfrac{\ln(1-z)}{z}$ for $z_1 = i$, $z_2 = 2 - i$, $z_3 = 4 - 3i$, $z_4 = -2 + 3i$ and $z_1^* = 1 + i$, $z_2^* = 1 - i$, $z_3^* = 1 + 3i$, $z_4^* = 1 - 3i$.

(iii) ***PAs of the inverted Stieltjes function.*** If f is a Stieltjes function, then the function g defined by

$$f(z) = \frac{f(0)}{1 - zg(z)}$$

is also a Stieltjes function and is called inverted function [1, 3, 4, 9, 10]. The inverted function to $f(z) = -\dfrac{\ln(1-z)}{z}$ is

$$g(z) = -\frac{1}{z} - \frac{1}{\ln(1-z)}.$$

The zeros and poles of PA $[n-1/n]$ and $[n/n]$ of g computed at $\zeta = i$ interlace in the vicinity of the straight line $[1, \infty[(i)$. It is a natural behavior indicating the cut chosen by PA (Fig. 25).

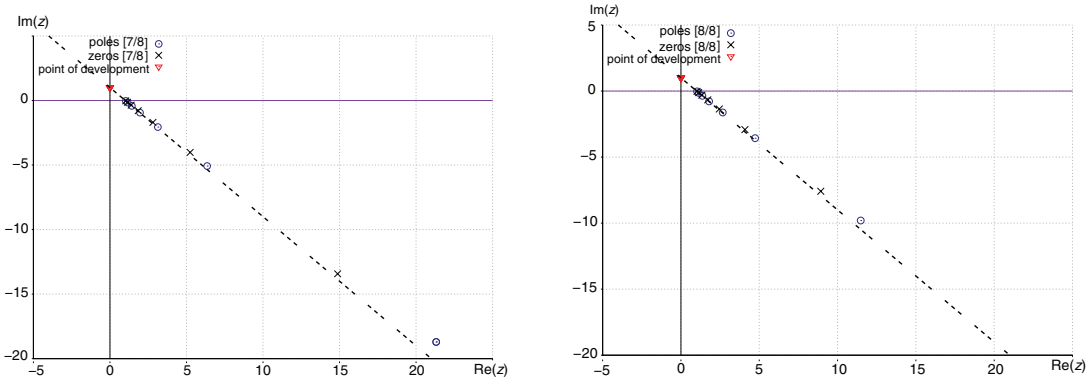

(*a*) (*b*)

Fig. 25. Distributions of zeros and poles of (*a*) PA [7/8] and (*b*) PA [8/8] computed at $\zeta = i$ to $g(z) = -\dfrac{1}{z} - \dfrac{1}{\ln(1-z)}$. Each line connects the point of development of $f : z = \zeta$ with the branch point $z = 1$.

7. Conclusions. Numerical experiments carried out with PA and NPA developed at the complex points revealed certain regularity related to their distribution of poles and zeros. It can be seen that positions of the poles and zeros for PA to the Stieltjes function expanded at $\zeta = ki$ (for numerically tested $k = \{0.2, \ldots, 10\}$) follow some well-defined corridors. In each case, they are included in a certain fan (i.e., regions having the shape of a wide "V") pointed on the ramification point R and directed by $[R, \infty[(R)$ line. When $k \to 0$ they lie on the real axis. An open question consists of determining the angles of this fan concerning the line $[R, \infty[(R)$ in each case. The paper also provides some new results relating to the distribution of zeros and poles of PA and NPA using the Taylor series of functions developed at the complex points and their conjugate points. The theorem for the case, when all the zeros and poles of NPA are real, is also formulated. It is derived on the base of the numerous numerical studies. We evidenced it in two cases [1/2] and [2/1] NPAs. At present many general problems in this field remain still open which can encourage the readers to solve them.

Appendix A. ***Exact solution for*** $\boldsymbol{[1/2]^{\mathbf{2}\,\mathbf{2}}_{\zeta,\overline{\zeta}}}$ **NPA** ***to*** $\boldsymbol{-\frac{1}{z}\ln(1-z)}$**.** This section provides the general solution for unknown coefficients a_0, a_1, b_1, b_2 which satisfy the matrix equation (8):

$$a_0 =$$

$$= \frac{\mathrm{Im}\,(\zeta)(c_0^2\overline{c_1}\overline{\zeta}\mathrm{Im}\,(\zeta) + c_1\zeta\,(\overline{c_0})^2\,\mathrm{Im}\,(\zeta) - 2c_0\overline{c_0}\mathrm{Im}\,(c_0)\mathrm{Re}\,(\zeta))}{\mathrm{Im}(\zeta(c_1\zeta+2c_0))\mathrm{Im}(\zeta(\mathrm{Re}(c_1\zeta)+\mathrm{Re}\,(c_0)-c_0))+\mathrm{Im}(c_1\zeta+c_0)\mathrm{Im}(\zeta(c_0\zeta-\mathrm{Re}(\zeta(c_1\zeta+2c_0))))},$$

$$a_1 =$$

$$= \frac{4c_0\,|c_0|^2\,(\mathrm{Re}\,(\zeta)-\zeta) - 4c_0^2\overline{c_1}\mathrm{Im}\,(\zeta)^2 + (\overline{c_0})^2\left(\zeta(c_1\zeta+4c_0) + c_1\overline{\zeta}\left(\overline{\zeta}-2\zeta\right) - 4c_0\mathrm{Re}\,(\zeta)\right)}{4(\mathrm{Im}(\zeta(c_1\zeta+2c_0))\mathrm{Im}(\zeta(\mathrm{Re}(c_1\zeta)+\mathrm{Re}(c_0)-c_0))+\mathrm{Im}(c_1\zeta+c_0)\mathrm{Im}(\zeta(c_0\zeta-\mathrm{Re}(\zeta(c_1\zeta+2c_0)))))},$$

$$b_1 =$$

$$= \frac{\mathrm{Im}\,(\zeta(c_1\zeta+2c_0))\mathrm{Im}\,(c_0-\zeta\mathrm{Re}\,(c_1)) + \mathrm{Im}\,(c_1)\mathrm{Im}\,(\zeta(\mathrm{Re}\,(\zeta(c_1\zeta+2c_0)) - c_0\zeta))}{\mathrm{Im}\,(\zeta(c_1\zeta+2c_0))\mathrm{Im}(\zeta(\mathrm{Re}(c_1\zeta)+\mathrm{Re}(c_0)-c_0))+\mathrm{Im}(c_1\zeta+c_0)\mathrm{Im}(\zeta(c_0\zeta-\mathrm{Re}(\zeta(c_1\zeta+2c_0))))},$$

$$b_2 =$$

$$= \frac{\mathrm{Im}\,((c_1\zeta+c_0)\mathrm{Im}\,(\zeta\mathrm{Re}\,(c_1)-c_0) + c_1\mathrm{Im}\,(\zeta(c_0-\mathrm{Re}\,(c_1\zeta+c_0))))}{\mathrm{Im}\,(\zeta(c_1\zeta+2c_0))\mathrm{Im}(\zeta(\mathrm{Re}(c_1\zeta)+\mathrm{Re}(c_0)-c_0))+\mathrm{Im}(c_1\zeta+c_0)\mathrm{Im}(\zeta(c_0\zeta-\mathrm{Re}(\zeta(c_1\zeta+2c_0))))}.$$

We present below the exact formulas for zero (ζ_0) and poles ($\zeta_1,\ \zeta_2$) of approximant.

The zero is obtained from the linear equation $a_0 + a_1\zeta_0 = 0$:

$$\zeta_0 = -\frac{4\mathrm{Im}\,(\zeta)\left(c_0^2\overline{c_1\zeta}\mathrm{Im}\,(\zeta) + c_1\zeta\,(\overline{c_0})^2\,\mathrm{Im}\,(\zeta) - 2c_0\overline{c_0}\mathrm{Im}\,(c_0)\mathrm{Re}\,(\zeta)\right)}{4c_0\,|c_0|^2\,(\mathrm{Re}\,(\zeta)-\zeta) - 4c_0^2\overline{c_1}\mathrm{Im}\,(\zeta)^2 + (\overline{c_0})^2\left(\zeta(c_1\zeta+4c_0) + c_1\overline{\zeta}\left(\overline{\zeta}-2\zeta\right) - 4c_0\mathrm{Re}\,(\zeta)\right)}$$

while the poles from the quadratic equation $1 + b_1\zeta + b_2\zeta^2 = 0$:

$$\zeta_1 = \frac{-b_1 - \sqrt{\Delta}}{2b_2}, \quad \zeta_2 = \frac{-b_1 + \sqrt{\Delta}}{2b_2},$$

where the discriminant of the quadratic equation is equal

$$\Delta = \frac{P(\zeta)}{Q(\zeta)},$$

$$P(\zeta) = (\mathrm{Im}\,(\zeta(c_1\zeta + 2c_0))\mathrm{Im}\,(c_0 - \zeta\mathrm{Re}\,(c_1)) + \mathrm{Im}\,(c_1)\mathrm{Im}\,(\zeta(\mathrm{Re}\,(\zeta(c_1\zeta + 2c_0)) - c_0\zeta)))^2 -$$

$$-4\,\mathrm{Im}\,((c_1\zeta + c_0)\mathrm{Im}\,(\zeta\mathrm{Re}\,(c_1) - c_0) + c_1\mathrm{Im}\,(\zeta(c_0 - \mathrm{Re}\,(c_1\zeta + c_0))))(\mathrm{Im}\,(\zeta(c_1\zeta +$$

$$+2c_0))\mathrm{Im}\,(\zeta(\mathrm{Re}\,(c_1\zeta) + \mathrm{Re}\,(c_0) - c_0)) + \mathrm{Im}\,(c_1\zeta + c_0)\mathrm{Im}\,(\zeta(c_0\zeta - \mathrm{Re}\,(\zeta(c_1\zeta + 2c_0))))),$$

$$Q(\zeta) = (\mathrm{Im}\,(\zeta(c_1\zeta + 2c_0))\mathrm{Im}\,(\zeta(\mathrm{Re}\,(c_1\zeta) + \mathrm{Re}\,(c_0) - c_0)) +$$

$$+\mathrm{Im}\,(c_1\zeta + c_0)\mathrm{Im}\,(\zeta(c_0\zeta - \mathrm{Re}\,(\zeta(c_1\zeta + 2c_0)))))^2,$$

$$c_0(\zeta) = -\frac{\ln(1-\zeta)}{\zeta},$$

$$c_1(\zeta) = \frac{1}{(1-\zeta)\zeta} + \frac{\ln(1-\zeta)}{\zeta^2}.$$

Those solutions are presented in Fig. 14 (*a*). To analyse the behavior of distributions zero and poles, we also chose the particular case of $\zeta = 1 + iy$ and $y > 0$. In this case, we obtain the relatively simple results.

$$a_0 = \frac{y(\pi^2(\pi y^2 - 4y + \pi) + 4(\pi y^2 + 4y + \pi)\ln^2(y) - 8\pi(y^2 - 1)\ln(y))}{(\pi^2 - 4)(y^2 + 1)^2},$$

$$a_1 = -\frac{y(\pi^2(\pi - 2y) + 4(2y + \pi)\ln^2(y) + 8\pi\ln(y))}{(\pi^2 - 4)(y^2 + 1)^2},$$

$$b_1 = -\frac{2(-2\pi y^3 + (\pi^2 - 4)y^2 + 2(\pi y^2 + 4y + \pi)y\ln(y) + 2\pi y + \pi^2 - 4)}{(\pi^2 - 4)(y^2 + 1)^2},$$

$$b_2 = \frac{-(4 + \pi^2)y^2 + 4\pi y + 4(2y + \pi)y\ln(y) + \pi^2 - 4}{(\pi^2 - 4)(y^2 + 1)^2}.$$

The zero is given by the equation

$$\zeta_0 = \frac{\pi^2(\pi y^2 - 4y + \pi) + 4(\pi y^2 + 4y + \pi)\ln^2(y) - 8\pi(y^2 - 1)\ln(y)}{\pi^2(\pi - 2y) + 4(2y + \pi)\ln^2(y) + 8\pi\ln(y)}$$

while the discriminant of the quadratic equation

$$\Delta = \frac{P_1(\zeta)}{(\pi^2 - 4)^2(y^2 + 1)^4},$$

$$P_1(\zeta) = 4((-2\pi y^3 + (\pi^2 - 4)y^2 + 2(\pi y^2 + 4y + \pi)y\ln(y) + 2\pi y + \pi^2 - 4)^2 -$$

$$-(\pi^2 - 4)(y^2 + 1)^2(-(4 + \pi^2)y^2 + 4\pi y + 4(2y + \pi)y\ln(y) + \pi^2 - 4)).$$

Those results are shown in Fig. 14 (*b*).

References

1. G. A. Baker Jr., *Essentials of Padé approximants*, Acad. Press, London (1975).
2. J. S. R. Chisholm, A. C. Genz, M. Pusterla, *A method for computing Feynman amplitudes with branch cuts*, J. Comput. and Appl. Math., **2**, 73 – 76 (1976)
3. J. Gilewicz, *Approximants de Padé*, Lect. Notes Math., **667**, Springer-Verlag (1978).
4. J. Gilewicz, M. Pindor, *On the relation between measures defining the Stieltjes and the inverted Stieltjes functions*, Ukr. J. Math., **62**, № 3, 327 – 331 (2010).
5. F. Hebhoub, *Approximants de Padé à N points avec le point à l'infini pour les fonctions de Stieltjes* (in French), Ph.D. thesis, Univ. Badji Mokhtar, Annaba (2011).
6. F. Hebhoub, L. Yushchenko, *On the zeros and poles of 1-point and N-point Padé approximants of complex-symetric functions in the case of the complex points*, Int. J. Math. and Math. Sci., Article ID 135481 (2011).
7. S. Klarsfeld, *Padé approximants and related methods for computing boundary values on cuts*, Lect. Notes Math., **888**, Springer, Berlin (1981), p. 255 – 262.
8. L. Yushchenko, *Approximants de Padé à N points complexes pour les fonctions de Stieltjes* (in French), Ph.D. thesis, Univ. de Toulon (2010).
9. J. Gilewicz, M. Pindor, S. Tokarzewski, J. J. Telega, *N-point Padé approximants and two sided estimates of errors on the real axis for the Stieltjes functions*, J. Comput. and Appl. Math., **178**, 247 – 253 (2005).
10. J. Gilewicz, *100 years of improvements of bounding properties of one-point, two-point and N-point Padé approximants to the Stieltjes functions*, Appl. Numer. Math., **60**, 1320 – 1331 (2010).
11. R. Jedynak, J. Gilewicz, *Approximation of smooth functions by weighted means of N-point Padé approximants*, Ukr. Math. J., **65**, № 11, 1566 – 1576 (2014).
12. R. Jedynak, *Approximation of the inverse Langevin function revisited*, Rheol. Acta, **54**, 29 – 39 (2015).
13. R. Jedynak, *New facts concerning the approximation of the inverse Langevin function*, J. Non-Newton Fluid, 8 – 25 (2017).
14. R. Jedynak, J. Gilewicz, *Magic efficiency of approximation of smooth functions by weighted means of two N-point Padé approximants*, Ukr. Mat. Zh., **70**, № 9, 1192 – 1210 (2018).

Received 17.09.18